MICROWAVE LAND EMISSIVITY MODEL DEVELOPED FOR SATELLITE DATA ASSIMILATION AND REMOTE SENSING APPLICATIONS

F. Weng

NOAA/NESDIS/Office of Research and Applications
Camp Springs, MD USA

Abstract - Satellite microwave measurements over land are strongly affected by surface emissivity and are presently not utilized for data assimilation studies because of the uncertainty in estimating the emissivity. This study develops a new model to quantify the land emissivity over various surface conditions. The volumetric scattering of surface materials is calculated using a two-stream approximation. The reflection and emission on surface boundaries are derived using Fresnel equations and further modified with cross-polarization and roughness factors. Geometric optics is used for the vegetation canopy to compute the optical parameters whereas a dense medium theory is further developed for snow and desert scatterers. A global distribution of land surface emissivity is simulated and compared with satellite retrievals from the Special Sensor Microwave Imager (SSM/I). The simulation and observation agree over most land conditions. However, larger discrepancies primarily occur at higher latitudes where the surface is covered by snow. This suggests that satellite retrieved emissivity may be needed to adjust the model results over these regimes.

1. INTRODUCTION

Measurements obtained from satellite passive microwave sensors are increasingly being utilized for improving the skill of numerical weather prediction (NWP). In 1998, National Atmospheric and Oceanic Administration (NOAA) launched its first Advanced Microwave Sounding Unit-A (AMSU-A) which includes 12 sounding channels in addition to 3 window channels. The sounding channels are located near 60 GHz oxygen absorption line and provide the capability of atmospheric temperature profiling under nearly all-weather conditions. Currently, the satellite measurements over ocean have been successfully utilized for many NWP models such as the global data assimilation system (GDAS) of National Environmental Center (EMC) of National Weather Service (NWS) (Errico et al. 2000). The impacts of the AMSU-A on forecasting and monitoring severe weather events such as hurricane are very remarkable (Weng et al., 2000; Zhu et al.; 2000). However, outstanding problems remain in using microwave sounding data over land and are caused by the variability of surface emissivity and its spectra which is largely unknown over many different surface conditions. The satellite data assimilation community has recently requested development of a microwave land emissivity model that can be directly implemented into the NWP models (Errico et al. 2000).

Microwave emissivity spectra were simulated and measured over limited land conditions. For a bare soil surface, the emissivity is derived as a function of soil moisture, soil textural components (e.g. clay and sand) and surface roughness (Choudhury et al. 1979; Wang and Schmugge 1980). However, the bare soil emissivity is modeled well at the lower frequencies where the dielectric constants are calibrated with the ground-based measurements. The emissivity of vegetation canopy was also simulated using a radiative transfer model and the canopy optical parameters are approximated by Rayleigh's approach (Mo et al. 1982). Recently, various sophisticated radiative transfer schemes were proposed to simulate the responses of microwave emissivity to canopy parameters (Wegmüller et al. 1995; Fung 1994; Kerr and Njoku 1990). For snow-covered surfaces having a high fraction volume of scattering particles, scattering and emission processed are approximated by a small perturbation theory which determines the effective wave propagation

constant (Tsang et al. 1985). Alternatively, Mie phase matrix was modified to account for scattering interaction of closely-spacing scatterers (Fung 1994). Recently, techniques were also proposed to retrieve the microwave emissivity over global land conditions using the Special Sensor Microwave Imager (SSM/I) and other auxiliary data (Jones and Vonder Haar 1997; Prigent et al. 1997). The retrieval is best performed at microwave window channels at lower frequencies where the needs for a correction of atmospheric emission are minimal (Prigent et al. 1997). However, the emissivity spectra can be only derived at satellite viewing angles. Since the satellite field of view varies with frequency, it is difficult to interpret the SSM/I derived emissivity spectra over a complex terrain, near coast lines, lakes and rivers without reducing all measurements to the largest satellite field of view (Jones and Vonder Haar 1997). Furthermore, the accuracy is very poor under severe weather conditions.

While microwave emissivity can be simulated for limited surface types, it is still questionable if the simulation accuracy can meet the operational purposes required in NWP data assimilation system. This study first presents a new land emissivity model. Simulated emissivity is then compared with satellite retrieval. The application of this model is finally illustrated.

2. EMISSIVITY MODEL

Microwave emissivity and its spectrum over land vary with surface conditions such as vegetation cover, flooding, and snow. Over densely vegetated areas, the emissivity is a function of leaf shape, vegetation density and canopy water content, frequency and polarization. Over snow-covered surfaces, the emissivity is primarily affected by the snow water equivalent content, age and particle size. The emissivity may also display variation on a spatial scale smaller than that resolved by current spaceborne microwave radiometers. An emissivity model was recently developed for various land conditions (Weng and Yan 2000). With this model, the emissivity can be calculated using various geophysical parameters such as vegetation cover, plant water content, soil moisture content and snow depth.

The land emissivity model was developed for following surface types: bare soil, desert sands, canopy and snow-covered conditions, as shown schematically in Fig. 1. Bare soil is treated as a slab having a rough surface. Within the slab, soil and solids are mixed according to their bulk densities. Furthermore, both compositions are made of clay and sand having respective fractions.

Canopy layer is characterized by an orientation distribution function and density distribution function of leaves. The leaves all have the same thickness. Since the leaf size is normally much larger than the wavelength of incident radiation, geometric optical theory can be used to compute the reflectivity and transmissivity. The leaf thickness affects the propagation phase of transmitted and reflected radiative components. The scattering and absorption coefficients of canopy layer are derived through integrating the optical parameters of all leaves distributed according to the orientation distribution function and density distribution function.

Desert sands and snow-covered surfaces are both considered as scattering material because a large fraction volume of particles are embedded within. For a scattering medium, particle diameter, fraction volume and medium depth are the most important parameters because they are directly related to particle optical parameters. Due to a higher fraction volume, the scattering of radiation from particles is partly coherent. Presently, this coherent effect is approximated by an effective wave-propagation constant.

When a surface layer contains scattering and absorbing material, various radiative components are involved in radiative transfer calculation. As shown in Fig. 1, the medium above the layer is the air containing no scatterers with a dielectric constant of ε_1 whereas the medium below the layer is homogeneous and characterized by a dielectric constant of ε_3. Since there is a discontinuity in the dielectric constant at the interface, radiative transfer processes should also include the surface reflection.
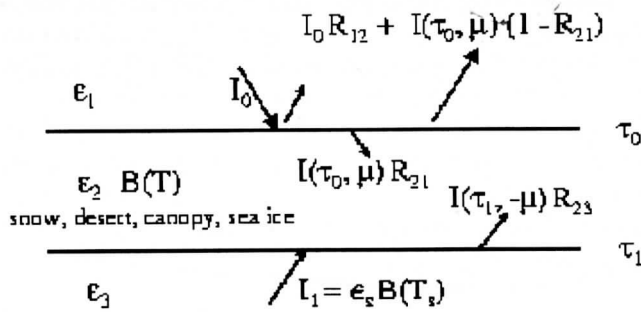
Figure 1. Radiative transfer process for various boundary layer materials. I_0 and I_1 are the incident radiative components from the atmosphere and the surface. B is the Planck function, T_s and T are the temperature for medium 2 and subsurface. R_{12} is the reflectivity from medium 1 to 2 whereas R_{21} is the reflectivity from medium 2 to 1. R_{23} are the reflectivity from medium 2 to 3. τ is the optical thickness and μ is the cosine of local zenith angle. ε is the dielectric constant.

The solution for the emissivity problem in Fig. 1 is derived at arbitrary viewing angles using the two-stream approximation (Weng and Yan 2000; Weng and Grody 2000). The emissivity of the entire boundary is approximated as a ratio of total radiance emanating from the medium to the thermal radiance which is calculated from Planck function with the physical temperature. As a result,

$$\varepsilon = \frac{(1 - \beta)(1 - R_{21})\left[1 + \gamma e^{-2\kappa(\tau_1 - \tau_0)}\right]}{(1 - \beta R_{21}) - (\beta - R_{21})\gamma e^{-2\kappa(\tau_1 - \tau_0)}} +$$
$$\frac{\alpha(1 - R_{12})(1 - R_{21})\left[\beta - \gamma e^{-2\kappa(\tau_1 - \tau_0)}\right]}{(1 - \beta R_{21}) - (\beta - R_{21})\gamma e^{-2\kappa(\tau_1 - \tau_0)}} + \qquad , \qquad (1)$$
$$\frac{\alpha R_{12}\left[(1 - \beta R_{21}) - (\beta - R_{21})\gamma e^{-2\kappa(\tau_1 - \tau_0)}\right]}{(1 - \beta R_{21}) - (\beta - R_{21})\gamma e^{-2\kappa(\tau_1 - \tau_0)}}$$

where α is the ratio of the incident radiation to the thermal emission by medium 2; $\beta = (1 - a)/(1 + a)$; $\gamma = (\beta - R_{23})/(1 - \beta R_{23})$; $\kappa^2 = (1 - \omega)(1 - \omega g)/\mu^2$; and a, ω, g, are the similarity parameter, single scattering albedo and asymmetry factor, respectively.

Generally speaking, the first term in Eq. (1) is associated with the scattering and emission from medium 2. The second term is due to the thermal radiation incident from medium 1 and is absorbed and re-emit by medium 2 whereas the third term is related to the interface reflection between medium 1 and 2. Since the reflectivity occurring at the interface is dependent on polarization, the emissivity derived from Eq. (1) may be also a function of polarization.

Since the surface boundary as shown in Fig. 1 normally is made of several media, the dielectric constant of the matrix can be specified using various mixing formulas. For example, a soil-water mixing formula was developed to calculate the effective dielectric constant (EDC) of bare soil (Dobson et al. 1985). However, earlier dielectric constant model of soil only yields an excellent fit to the experimental data for frequencies less than 5 GHz.

Canopy leaves are also considered as a matrix containing dry matter and water. Since the EDC generally decreases as canopy gravimetric water content increases, the leaves of green canopy have higher EDC than yellow leaves because of their higher amount of gravimetric water content. A dielectric constant model of

leaves developed by Mätzler (1994) is used to compute the optical parameters of canopy. As shown in Fig. 2, the single scattering albedo is normally with 0.3 and 0.5 and is not negligible. The albedo increases as the leaf thickness increases and as the frequency increases. This result may imply that the intensity of canopy scattering may be pronounced at high frequencies and should be explicitly included in the radiative transfer process.
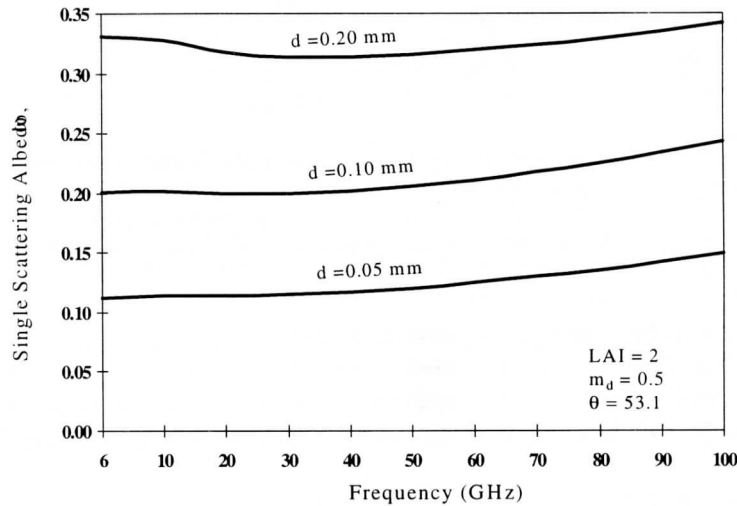

Figure 2. Canopy single scattering albedo as a function of frequency with a leaf thickness (d) as a parameter. LAI is the leaf area index; m_d is the dry matter content; and ϑ is the local zenith angle.

The EDC for snow particle and desert sands is derived using a small perturbation theory (Weng and Yan, 2000) as a linear function of the volume fraction that the particles occupy. Resulting EDC increases as the volume fraction increases. With this EDC model, the optical thickness and single scattering albedo of snow are computed as a function of frequency with the volume fraction as a parameter. As shown in Fig. 3, the single scattering albedo increases dramatically as the frequency increases for a volume fraction less than 0.3. However, for a fraction volume greater than 0.9, the albedo is much lower and almost independent of the frequency. This albedo depression is part of the dense medium effects.

When the surface of bare soil is smooth, the emissivity can be directly calculated using Fresnel equations with the effective dielectric constant discussed above. However, as the surface becomes rough, the results from Fresnel equations is modified by an exponential function of the roughness height and further adjusted by a cross-polarization factor that is also a function of the roughness height.

Figures 4a - 4d display simulated bare soil emissivity as a function of volumetric moisture content at four individual frequencies. Apparently, the emissivity for all frequencies decreases as the soil moisture content increases. As expected, the lowest frequency displays the largest sensitivity to the soil moisture.

For a canopy-covered surface, the sensitivity of emissivity to soil moisture is significantly reduced. As shown in Figs. 5a – 5d, the emissivity at frequencies higher than 19.35 GHz is almost independent of the soil moisture when the canopy gravimetric water content is 0.5 kg/m^2. However, the emissivity at frequencies less than 10.6 GHz is still sensitive to soil moisture.
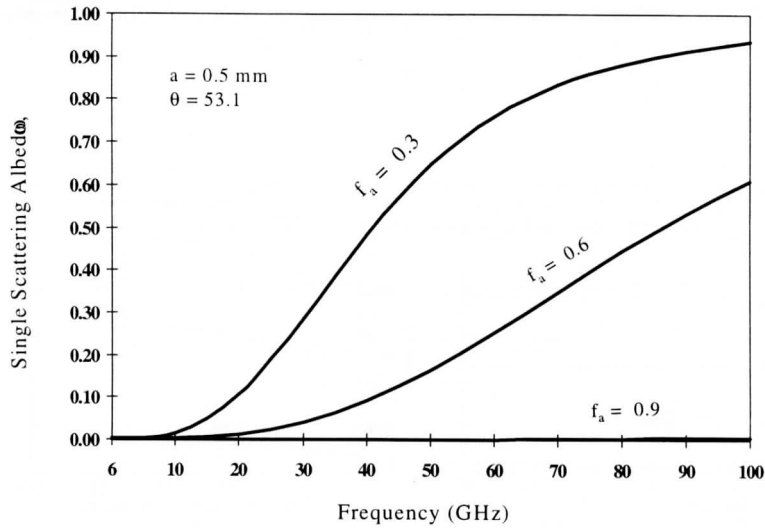
Figure 3. Single scattering albedo of snow as a function of frequency. f_a is the volume fraction and a is the mean particle radius.
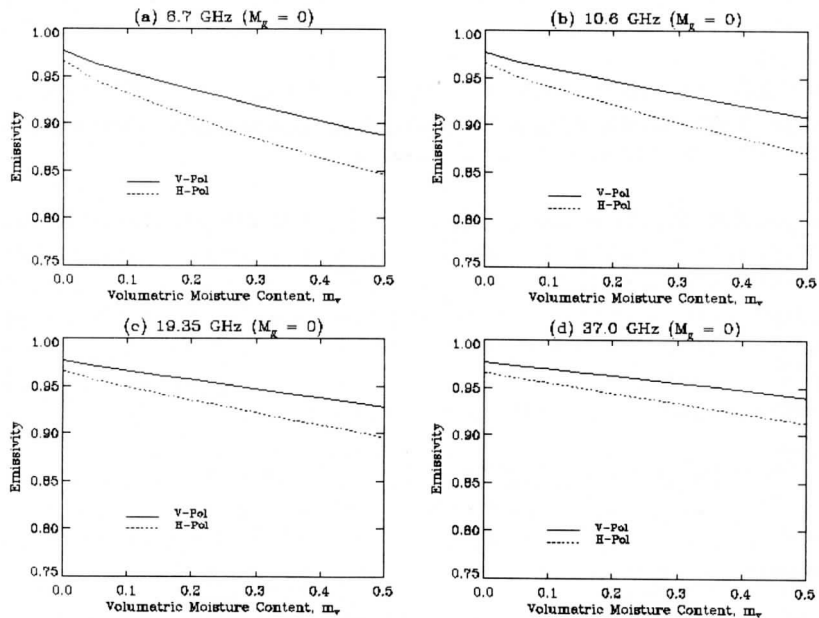

Figure 4. Emissivity vs. volumetric soil moisture content. M_g is the canopy water content and is specified to zero for representing a bare soil condition.
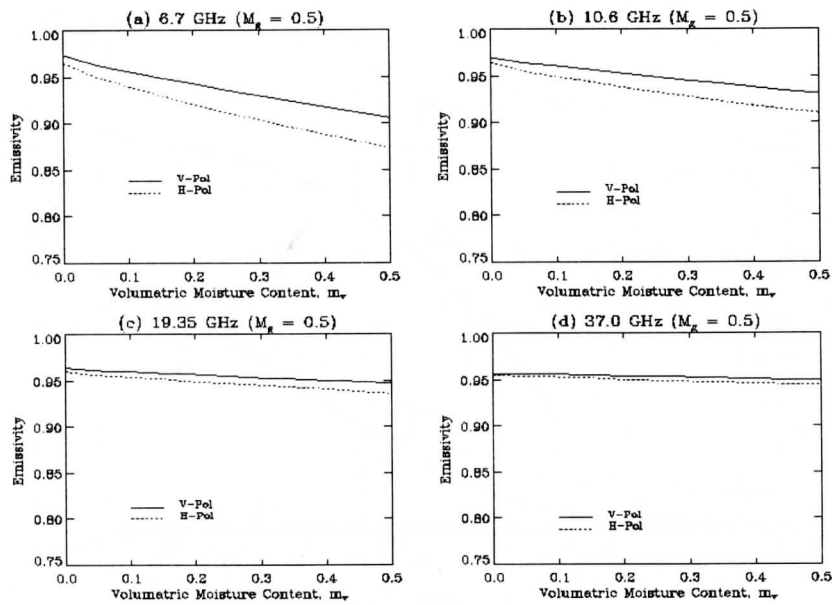
427

Figure 5. Emissivity vs. volumetric soil moisture content. M_g is set as 0.5 kg/m^2 for representing vegetation-covered soil condition.

Figures 6a - 6d display the emissivity in relation to the canopy water content. In general, the emissivity decreases as the canopy water content increases. In particular, the emissivity at 85.5 GHz has the largest sensitivity due probably to an increasing scattering albedo (see Fig. 2).

Figures 7a -7d show the emissivity for a snow-covered surface as a function of snow depth. Evidently, the emissivity at 85.5 GHz is the most sensitive to the snow depth.
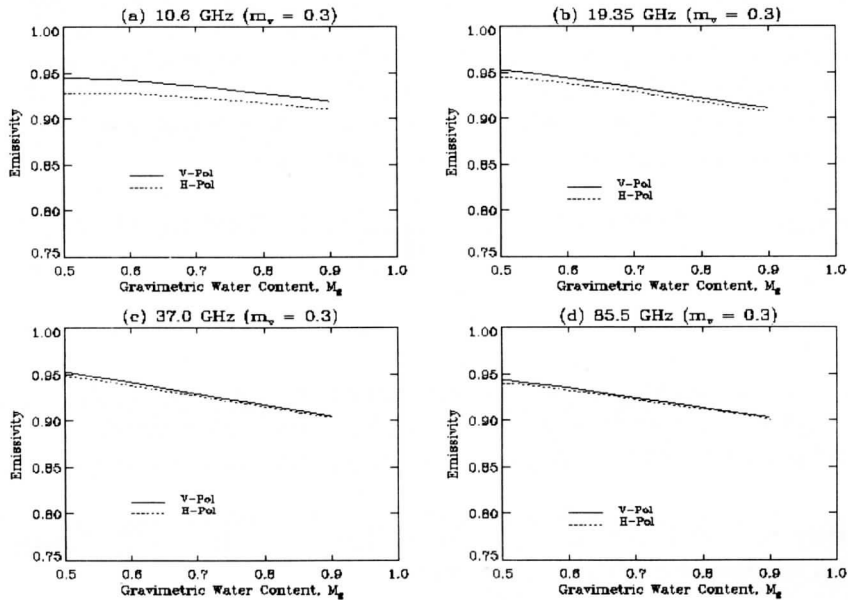

Figure 6. Emissivity vs canopy gravimetric water content. m_v is the volumetric soil moisture content.
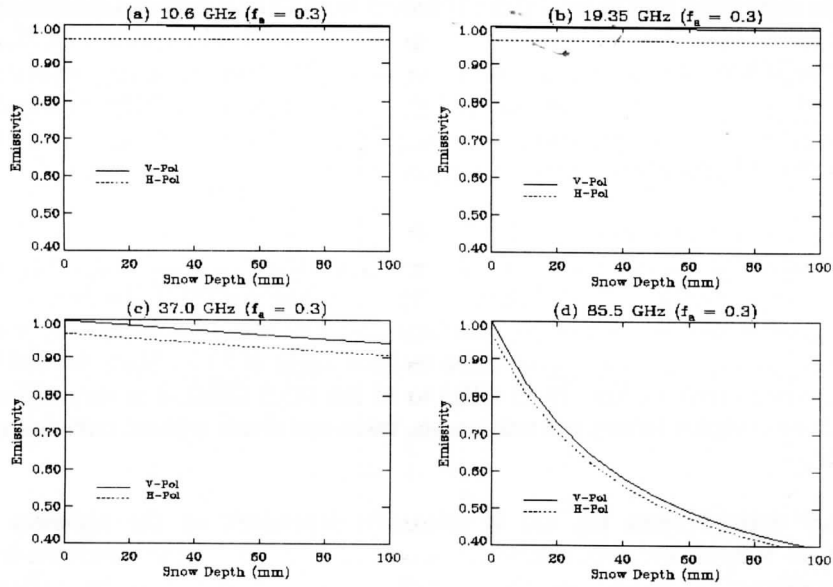
Figure 7. Emissivity vs. snow depth. f_a is the volume fraction which is set to 0.3, representing newly formed snow on the ground.

3. MICROWAVE EMISSIVITY RETRIEVAL

Land emissivity can be directly retrieved from satellite observations if the atmospheric emission and scattering components are quantified and removed from the measurements. The retrieval method in this study is similar to those discussed by Prigent et al. (1997) and Jones and Vonder Haar (1997). In doing so, temperature and moisture profiles are obtained from the National Center for Environmental Prediction (NCEP) Global Data Assimilation System (GDAS) and used to compute atmospheric upwelling and downwelling radiative components and transmittance. Currently, the GDAS assimilated various data such as radiosonde measurements, satellite retrievals and forecast models to produce the reliable information on atmospheric temperature and moisture profile. Even over the areas where direct measurements are sparsely distributed or not available, the GDAS produces the estimates which are mainly based on the physical parameterization and dynamics of global numerical weather prediction model.

For a scattering-free atmosphere, the brightness temperature, T_b at the top of the atmosphere can be approximated as

$$T_b = T_{bu} + \tau\left[\varepsilon T_s + (1 - \varepsilon)T_{bd}\right], \tag{2}$$

where ε is the surface emissivity; T_s is the surface skin temperature; τ is the atmospheric transmittance; T_{bu} and T_{bd} are the brightness temperatures at upwelling and downwelling directions, respectively. The dependence on polarization, frequency and angle in Eq. (2) is suppressed for simplicity.

Using Eq. (2), one can solve for surface emissivity as a function of above parameters, i.e.,

$$\varepsilon = \frac{T_b - T_u - T_d\tau}{\tau(T_s - T_d)}, \tag{3}$$

The variables on the right hand side in Eq. (3) are obtained from GDAS data and satellite measurements. In particular, T_b is from the Special Sensor Microwave Imager (SSM/I). The parameters, T_{bu}, T_{bd}, and τ are computed using the NCEP GDAS outputs. These variables however must be co-located with satellite measurements in both space and time. First, the SSM/I measurements are spatially matched with the GDAS data sets including atmospheric temperature, moisture profiles and surface temperature. Then, the GDAS analyses at 00, 06, 12 and 18Z are interpolated to obtain the values near the time of satellite observations.

Retrieved emissivity can be only obtained at the SSM/I frequencies and polarization, Earth incidence angle (EIA) and spatial resolutions. The SSM/I is a seven-channel radiometer having frequencies at 19.35, 22.235, 37.0 and 85.5 GHz. Each channel has both vertical (V) and horizontal (H) polarization except the 22.235 GHz channel, which measures only vertically - polarized radiation. The SSM/I conically scans the Earth and atmosphere with an angle of 45^0 resulting in an Earth incident angle of 53.1^0. Since the SSM/I effective field of view (EFOV) decreases from 60 km (19.35 GHz) to 15 km (85.5 GHz), it is very difficult to obtain the emissivity spectra for a complex terrain and near coasts, lakes and rivers without reducing all measurements to the largest EFOV.

Emissivity accuracy derived from Eq. (3) is primarily dependent on the accuracy of atmospheric transmittance, surface temperature and brightness temperature. Under clear atmospheric conditions, the errors in the transmittance are mainly resulted from the errors in water vapor absorption model and the GDAS water vapor profile. Various analyses have indicated that the present water vapor absorption models may contain an uncertainty as large as 10% – 15% for the water vapor absorption coefficient, particularly at 22 and 85 GHz (Prigent et al. 1997). This alone could result in an error of 2% – 5% in emissivity retrieval. Presently, the error of the GDAS water vapor profiles is largely unknown. Thus, the actual usefulness of the retrieved emissivity at SSM/I 22.235 and 85.5 GHz remains highly questionable, especially for the areas where the radiosonde observations are very limited.

Since the surface temperature in Eq. (3) is approximated by GDAS shelter-air temperature, additional errors in emissivity retrieval may also result. However, this error magnitude is limited within 1% when the SSM/I measurements from morning pass orbits are used in retrievals. This is because the energy exchange between the surface and lower atmosphere reaches a balance during morning and thus the difference between surface and shelter air temperatures is less than 2 K (Weng and Grody 1998).

The emissivity is currently derived under cloud-free conditions. Clouds within the SSM/I EFOV are identified using satellite infrared measurements. A threshold of 22 K based on the difference between GDAS surface temperature and the IR brightness temperature is used to detect the clouds within the SSM/I EFOV. However, low clouds or thin cirrus may be still undetected and result in some uncertainty in retrieved emissivity.

Multiple satellite orbits are used to produce a composite emissivity data set over land. When single SSM/I instrument is utilized, the composite map requires the data during a week so that the most of land areas can be covered with retrievals. However, for those areas (e.g. Amazon basin) where clouds and precipitation prevail, the composite needs the observations for a longer time of period (e.g. half month).

Figures 8a - 8c show the mean vertically polarized land emissivity at the SSM/I frequencies of 19.35, 37.0 and 85.5 GHz for March 1999 whereas Figs. 9a - 9c show corresponding polarization difference. Apparently, the emissivity varies substantially from region to region. Snow displays a lowest emissivity and highest polarization difference and its spectra vary according to the age of the snow-pack and sub-surface stratification. For example, snow over northern and central Greenland produces a much lower emissivity (< 0.7) and higher polarization difference (> 0.2) at 19.35 GHz, compared to that observed over North America and North Europe. This may be associated with a deep layer of snow that is vertically stratified.
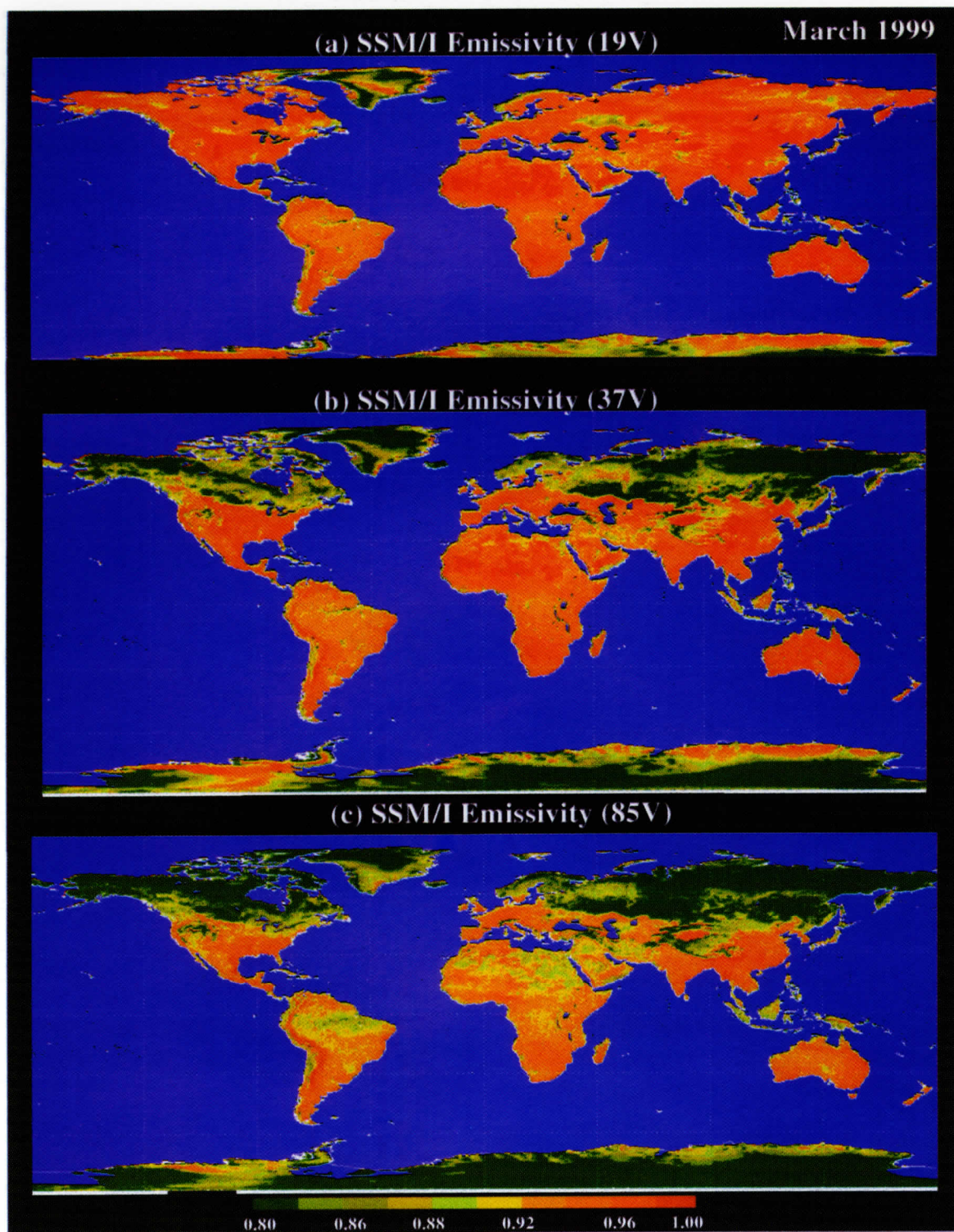
Figure 8. Microwave land emissivity at (a) 19.35 GHz, (b) 37 GHz and (c) 85.5 GHz retrieved from the SSM/I
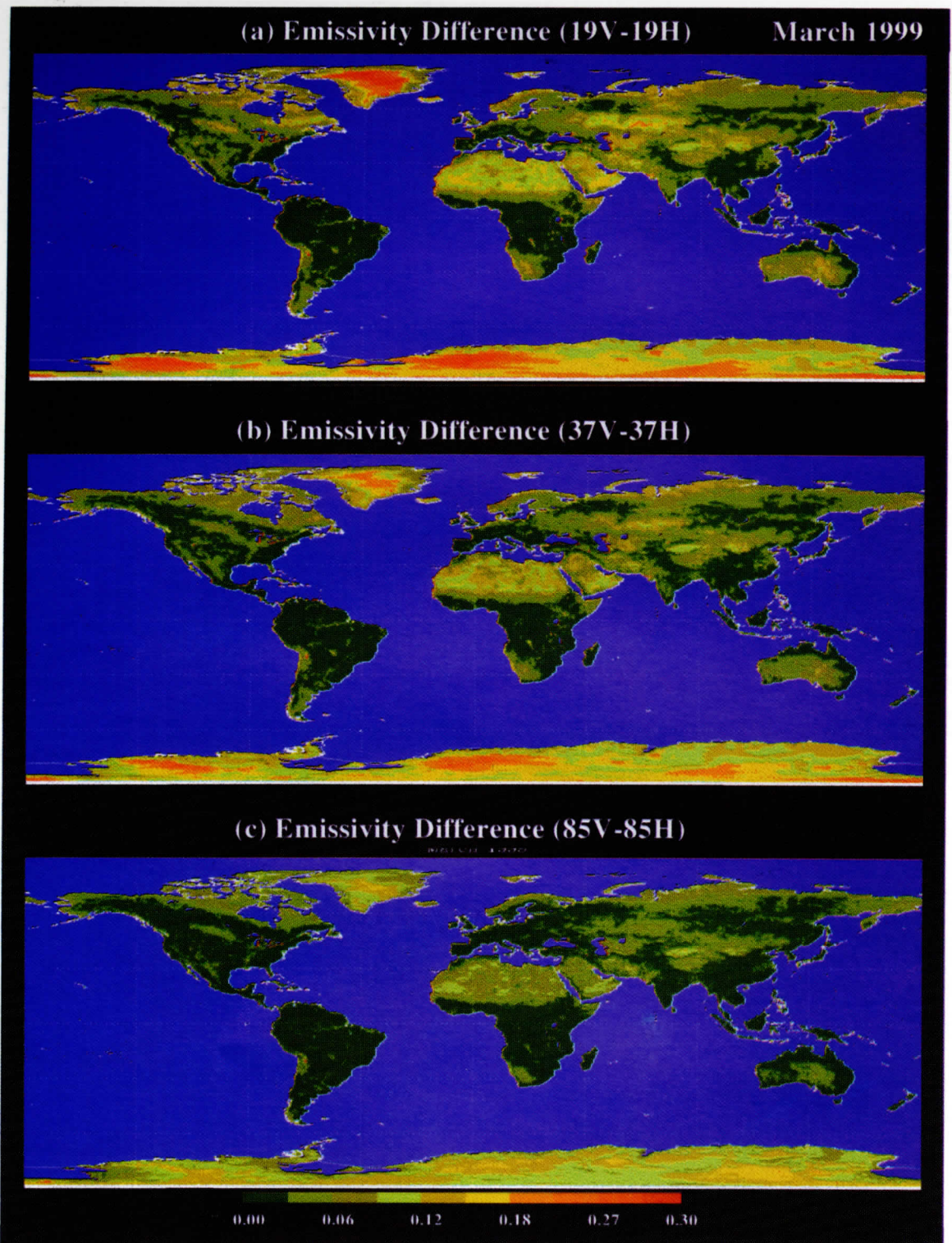
Figure 9. Polarization difference in microwave land emissivity retrieved from the SSM/I.

The emissivity derived from the models can be directly compared with satellite retrievals so that the fidelity of the model may be established. A simulation of global emissivity requires the parameters,

432

vegetation types, canopy gravimatric water content, snow depth, and soil moisture content and so on. Many of these parameters are available from the GDAS. The GDAS also predicts some surface parameters such as canopy water content, soil moisture content, skin and soil temperature from its boundary layer model. This study uses all possible information regarding the land surface from the GDAS to categorize the surface types that are radometrically consistent with the emissivity model. However, some parameters such as particle size and leaf thickness remain unknown although they are very important to the emissivity model. Presently, the radius of the dense medium particles is set to 0.5 mm for snow and 1.0 mm for desert sand particles. The canopy leaf thickness is set to 0.02 mm. The uncertainty in specifying these parameters as the model inputs may be one of major error sources in simulated emissivity.

Figures 10a - 10b compares simulated emissivity with the SSM/I retrievals as shown in Figs. 10c-10d. While overall patterns are agreeable very well, the problems remains significant at higher frequencies and in polar areas. We are still facing a fundamental difficulty formulating an emissivity model including snow stratification and multiple scattering.
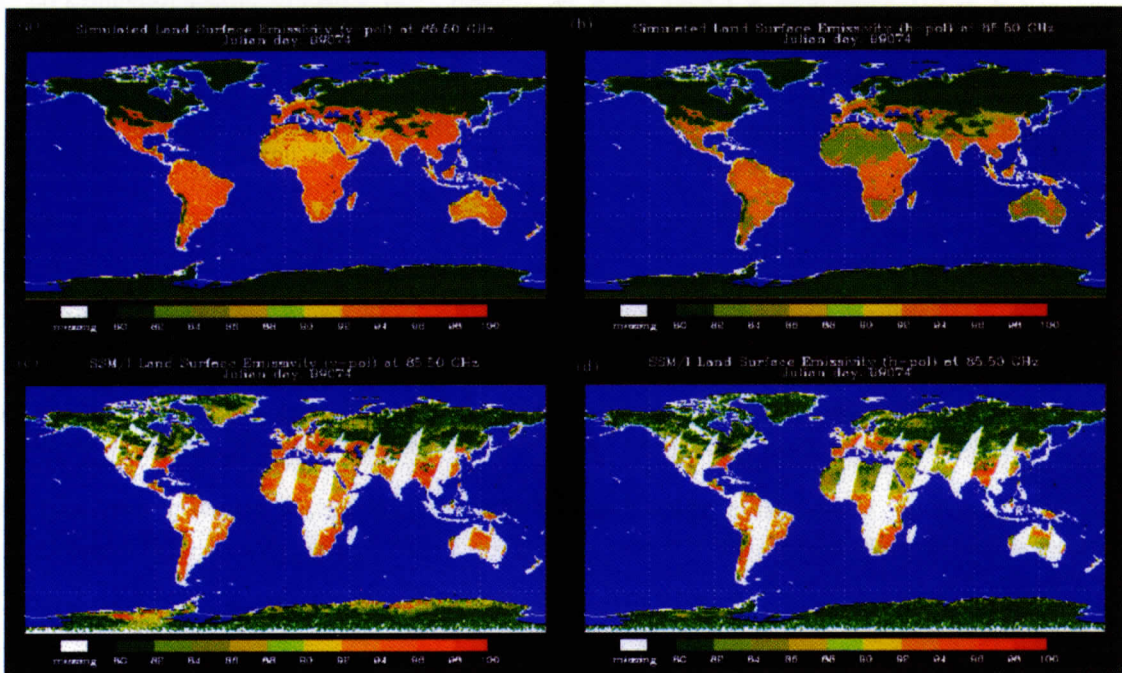

Figure 10. Simulated emissivity vs retrieved emissivity at 85.5 GHz for vertical polarization (a) and (c); and for horizontal polarization for (b) and (d).

4. Conclusions

This study presents a microwave land emissivity model that includes the emission and scattering process of various surface materials such as snow, desert and canopy leaves. The reflection and emission occurring on the interfaces above and below the scattering layer is also taken into account. Furthermore, the cross polarization and attenuation due to surface roughness are also parameterized as a function of roughness height and wavelength. For canopy leaves, the optical parameters are derived using the geometric optics because their sizes are typically larger than the wavelength. For a medium having a higher volume fraction of particles such as snow and desert, the scattering and absorption coefficients are approximated by a small perturbation theory.

433

Global land emissivity is simulated at 85.5 GHz and compared with the retrievals derived from the SSM/I. The retrieval algorithm is similar to the method of Prigent et al. (1997), except using temperature and moisture profile data from the NCEP global data assimilation system (GDAS). The GDAS currently assimilates various satellite and conventional observations and predicts various parameters such as canopy gravimetric water content, soil moisture content and snow depth from its boundary layer scheme. These parameters in conjunction with other observational data such as soil type and vegetation types are used as the inputs to the emissivity model. The global emissivity shows a reasonable pattern, compared to the satellite retrievals.

The present emissivity model can be further improved to include the vertical stratification of various scattering materials. The procedure of computing the optical parameters can be expanded to include more surface types. For the canopy layer containing the crop stems and tree trunks producing anisotropic scattering, more radiative transfer streams may be needed to accurately compute the scattering components in the model.

5. References

Choudhury, B. J, T. J. Schmugge, A. Chang and R.W. Newton, 1979: Effect of surface roughness on the microwave emission from soils, J. Geophys. Res., 84, 5699 - 5706.

Dobson, M. C., F. T. Ulaby, M. T. Hallinkainen, and M. A. El-Rayes, 1985: Microwave dielectric behavior of wet soil - part II: Dielectric mixing models, IEEE Trans. Geo. Remote Sensing, 25, 541 - 549.

Errico, R. and co-authors, 2000: NOAA/NASA/DoD workshop on satellite data assimilation Submitted to Bull Amer. Meteor. Soc.

Fung, A. K., 1994 : Microwave scattering and emission models and their applications, Artech House, Boston, MA. pp. 419-423.

Kerr, Y. H. and E. G. Njoku, 1990: A semi-empirical model for interpreting microwave emission from semiarid land surface as seen from space. *IEEE Trans. Geosci. Remote Sensing*, GE-28 (3), 384 - 393.

Jones, A. S. and T. H. Vonder Haar, 1997: Retrieval of microwave surface emittance over land using coincident microwave and infrared satellite measurements, J. Geophys. Res., 102 , 13, 609 - 13,626.

Mätzler, C., 1994: Microwave (1-100 GHz) dielectric model of leaves, *IEEE Trans. Geo. Remote Sensing*, 32, 947 - 949.

Mo, T., B. J. Choudhury, T. J. Schmuge, and J. R. Wang, 1982: A model for microwave emission from vegetation-covered fields, J. Geophy. Res., 87, 11,229 - 11,237.

Prigent, C., W. B. Rossow and E. Mattews, 1997: Microwave land surface emissvities estimated from SSM/I observations, J. Geophys. Res., 102, 867 - 890.

Tsang, L., J. A. Kong, R. T. Shin, 1985: Theory of microwave remote sensing. John Wiley & Sons, Inc. New York, p. 498.

Wang, J. R. and T. T. Schmugge, 1980: An empirical model for the complex dielectric permativity of soils as a function of water content, IEEE Trans. Geo. Remote Sensing, 18, 288 - 295.

Wegmüller, U., C. Mätzler, and E. Njoko, 1995: Canopy opacity models, *Passive microwave remote sensing of land-atmosphere interactions*, Eds, B. J. Choudhury, Y. H. Kerr, E. G. Njoko, and P. Pampaloni, VSP BV, Utrecht, The Nethelands, 380 - 384.

Weng, F. and N. C. Grody, 1998: Physical retrieval of land surface temperature using the special sensor microwave imager, *J. Geophys. Res.*, 103, 8839-8848.

Weng, F. and N. C. Grody, 2000: Retrieval of ice cloud parameters using a microwave imaging radiometer, J. Atmos. Sci., 57, 1069 - 1081

Weng, F. and B. Yan, 2000: Developments of Microwave land emissivity model and data sets for satellite data assimilation and remote sensing application, *J. Geophys. Res. (Revised)*

Weng, F., T. Zhu and D. Zhang, 2000: Applications of Advanced Microwave Sounding Unit to improving the analysis of atmospheric wind field in tropical cyclones, Preprint of the Fourth Symposium on Integrated Observing System, Amer. Meteor. Soc., Long Beach, CA.

Zhu, T, F. Weng and D. Zhang, 2000: An initialization scheme of hurricane model using the Advanced Microwave Sounding Unit measurement, *Mon Weather Rev. (Submitted)*

TECHNICAL PROCEEDINGS OF THE ELEVENTH INTERNATIONAL ATOVS STUDY CONFERENCE

Budapest Hungary

20-26 September, 2000

Edited by

J.F. Le Marshall and J.D. Jasper

Bureau of Meteorology Research Centre, Melbourne, Australia

Published by

Bureau of Meteorology Research Centre

PO BOX 1289K, GPO Melbourne, Vic., 3001, Australia

June 2001